

Respiratory Rate Estimation Based on WiFi Frame Capture

Takamochi Kanda*, Takashi Sato*[†], Hiromitsu Awano*[‡], Sota Kondo*, and Koji Yamamoto*[§]
*Graduate School of Informatics, Kyoto University, Yoshida-honmachi, Sakyo-ku, Kyoto, 606-8501, Japan
[†]takashi@i.kyoto-u.ac.jp, [‡]awano@i.kyoto-u.ac.jp, [§]kyamamoto@i.kyoto-u.ac.jp

Abstract—This paper presents a method that estimates the respiratory rate based on the frame capturing of wireless local area networks. The method uses beamforming feedback matrices (BFMs) contained in the captured frames, which is a rotation matrix of channel state information (CSI). BFMs are transmitted unencrypted and easily obtained using frame capturing, requiring no specific firmware or WiFi chipsets, unlike the methods that use CSI. Such properties of BFMs allow us to apply frame capturing to various sensing tasks, e.g., vital sensing. In the proposed method, principal component analysis is applied to BFMs to isolate the effect of the chest movement of the subject, and then, discrete Fourier transform is performed to extract respiratory rates in a frequency domain. Experimental evaluation results confirm that the frame-capture-based respiratory rate estimation can achieve estimation error lower than 3.2 breaths/minute.

I. INTRODUCTION

Monitoring vital signs, e.g., heart rate or respiratory rate, plays an important role in medical care, particularly after the global outbreak of COVID-19. Patients with serious symptoms need to constantly monitor their vital signs because their symptoms may suddenly worsen as observed in COVID-19 cases [1] or acute respiratory distress syndrome (ARDS) [2]. In recent times, the continuous sensing of biological signals relies on wired devices, which have been a burden for patients wearing them. One solution to realize contact-less vital sensing uses millimeter-wave radar [3]. However, it requires radar transmitters and receivers, which significantly increases the initial cost.

To alleviate this problem, vital sensing using WiFi devices has been installed in several places and is attracting a lot of attention. Conventionally, WiFi-based vital sensing relies on the received signal strength indicator (RSSI), which represents the received signal strength measured for each frame. However, owing to the low frequency and time resolution of RSSI, in recent years, the methods that use channel state information (CSI) has been proposed [4], [5]. The CSI carries channel information for each subcarrier as a multidimensional matrix. Owing to fine-grained channel information provided by CSI, respiratory rate [6], [7] and heart rate [8] can be accurately measured. Although the CSI-based approaches require no additional devices, retrieving CSI information requires firmware modifications or dedicated WiFi chipsets, which limit the applicability of CSI-based vital sensing.

Another promising technique is a frame-capture-based approach that uses beamforming feedback matrices (BFMs)

defined in IEEE 802.11ac/ax standard [9], [10]. For example, frame-capture-based indoor localization and outdoor human detection have been implemented using machine learning techniques [11]–[13]. Beamforming feedback frames that deliver BFMs can be easily captured by third parties because they are unencrypted. Moreover, capturing beamforming feedback frames does not require any special firmware or WiFi chipsets, which would have been necessary to obtain CSI. These facts can extend the applicability of frame capturing to various sensing tasks.

In this paper, we propose a respiratory rate estimation method and demonstrate the feasibility of vital sign monitoring based on frame capturing. Assuming that the chest movement owing to respiration is the dominant cause of signal fluctuation, first, principal component analysis (PCA) is applied to BFMs. Then, a discrete Fourier transform (DFT) is performed to extract the respiratory rate in the frequency domain.

The main contributions of this paper are summarized as follows:

- We propose a frame-capture-based respiratory rate estimation, which extends the applicability of WiFi-based vital sensing. The proposed method does not rely on any learning-based algorithms, and hence, it can be applied to various environments without incurring any cost related to learning. More specifically, we isolate the effect of chest fluctuation of the subject from other channel information by applying PCA to the captured BFMs and perform DFT on the first principal component to extract the periodic change in the signal caused by human breathing.
- We show the feasibility of accurate respiratory rate estimation based on frame capturing without specific firmware modifications or WiFi chipsets through experiments. The experimental results confirm that the proposed method can achieve estimation error lower than 3.2 breaths/minute.

The rest of this paper is organized as follows: Section II describes a system model and BFMs in the captured frames. Section III explains the proposed frame-capture-based respiratory rate estimation method. Section IV describes experimental evaluation results and discusses the results. Section V concludes the paper.

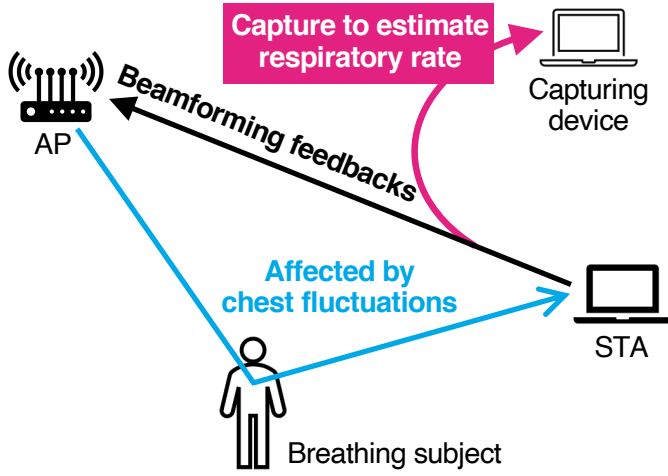


Fig. 1. Frame-capture-based respiratory estimation system. The STA transmits beamforming feedback frames to the AP, and the capturing device captures these frames to estimate the subject's respiratory rate.

II. SYSTEM MODEL

Fig. 1 shows the proposed respiratory rate estimation system based on frame capturing. The system comprises an access point (AP) with N_{AP} antennas, a station (STA) with N_{STA} antennas, and a capturing device, where we assume $N_{AP} \geq N_{STA}$. One subject breathes at rest in the vicinity of the AP and STA. The STA is associated with the AP, and the AP periodically transmits data frames to the STA. The capturing device captures the transmitted frames by the STA.

We exploit the beamforming feedback frames transmitted periodically from the STA to the AP according to the beamforming feedback procedure defined in IEEE 802.11ac/ax for the respiratory rate estimation. The beamforming feedback frames contain the elements of the BFM, $\mathbf{V} \in \mathbb{C}^{N_{AP} \times N_{STA}}$, which is defined as the right singular matrix of the CSI matrix $\mathbf{H} \in \mathbb{C}^{N_{STA} \times N_{AP}}$:

$$\mathbf{H} = \mathbf{U} \mathbf{\Sigma} \mathbf{V}^H, \quad (1)$$

$$\mathbf{y} = \mathbf{H} \mathbf{x}, \quad (2)$$

where $\mathbf{y} \in \mathbb{C}^{N_{STA}}$ and $\mathbf{x} \in \mathbb{C}^{N_{AP}}$ are the receive and transmit signal vectors, respectively, $\mathbf{U} \in \mathbb{C}^{N_{STA} \times N_{STA}}$ is the left singular matrix, $\mathbf{\Sigma} \in \mathbb{C}^{N_{STA} \times N_{STA}}$ is the diagonal matrix whose entries are singular values, and the superscript H denotes the Hermitian transpose.

As the elements of BFMs are transmitted in a compressed form, decompression is firstly performed before applying our respiratory rate estimation procedure. More concretely, BFM \mathbf{V} is expressed by $\phi_{i,j} \in [0, 2\pi]$, $\psi_{i,j} \in [0, \pi/2]$ based on Givens rotation as referred to in IEEE 802.11ac standard [9]:

$$\mathbf{V} = \left[\prod_{i=1}^{\min\{N_{AP}, N_{STA}-1\}} \mathbf{D}_i \left(\prod_{l=i+1}^{N_{STA}} \mathbf{G}_{l,i}(\psi_{l,i})^T \right) \right] \tilde{\mathbf{I}}_{N_{AP} \times N_{STA}}, \quad (3)$$

where

$$\mathbf{D}_i := \begin{bmatrix} \mathbf{I}_{i-1} & 0 & \cdots & \cdots & 0 \\ 0 & e^{j\phi_{i,i}} & 0 & \cdots & 0 \\ \vdots & 0 & \ddots & 0 & 0 \\ \vdots & \vdots & 0 & e^{j\phi_{N_{AP}-1,i}} & 0 \\ 0 & 0 & 0 & 0 & 1 \end{bmatrix} \quad (4)$$

is the diagonal matrix and

$$\mathbf{G}_{l,i}(\psi) := \begin{bmatrix} \mathbf{I}_{i-1} & 0 & 0 & 0 & 0 \\ 0 & \cos \psi & 0 & \sin \psi & 0 \\ 0 & 0 & \mathbf{I}_{l-i-1} & 0 & 0 \\ 0 & -\sin \psi & 0 & \cos \psi & 0 \\ 0 & 0 & 0 & 0 & \mathbf{I}_{N_{AP}-l} \end{bmatrix} \quad (5)$$

is the Givens rotation matrix. In these equations, $\tilde{\mathbf{I}}$ denotes the rectangular version of the identity matrix \mathbf{I} , i.e., main diagonal is 1 and other elements are represented by 0. In addition, $\phi_{i,j}$ and $\psi_{i,j}$ are respectively quantized to b_ϕ and b_ψ bits as

$$\phi_{i,j} = \frac{k_{\phi_{i,j}} \pi}{2^{b_\phi-1}} + \frac{\pi}{2^{b_\phi}}, \quad \psi_{i,j} = \frac{k_{\psi_{i,j}} \pi}{2^{b_\psi+1}} + \frac{\pi}{2^{b_\psi+2}}, \quad (6)$$

which are termed compressed BFMs.

III. FRAME-CAPTURE-BASED RESPIRATORY RATE ESTIMATION

We describe the overview of our frame-capture-based respiratory rate estimation method below. First, we isolate the effect of the chest fluctuation of the subject from other channel information by applying PCA to the decompressed data. Second, DFT is performed on the first principal component to extract the periodic change in the signal caused by human breathing, and finally, the respiratory rate is estimated by detecting the peak in the DFT signal. The details of each step are as follows:

Preprocessing. The decompressed BFM data is processed by a time window. Respiratory rate is estimated in real time by moving the time window in a constant interval so that it overlaps the adjacent time window. To apply PCA, the captured data is arranged two-dimensionally as a matrix of size $N_{\text{frame}} \times N_{STA} N_{AP} N_{sc}$ as shown in Fig. 2, where N_{frame} is the number of frames in the time window and N_{sc} is the number of subcarriers. We use the amplitude of decompressed BFMs rather than phase because the preliminary experiments confirmed that the amplitude of BFM synchronizes better with the subject's chest movement than the phase.

Second, we apply PCA to the data to separate the effect of chest movement from other channel information. We use the first principal component that most reflects the chest movement. Finally, we linearly interpolate the data to equalize the time intervals before performing DFT in the subsequent steps. Fig. 2 shows changes in data shape based on the preprocessing procedure, wherein N_{interp} denotes the number of interpolated points.

Respiratory Rate Estimation. We then extract the respiratory rate as the peak frequency of the DFT output. In order

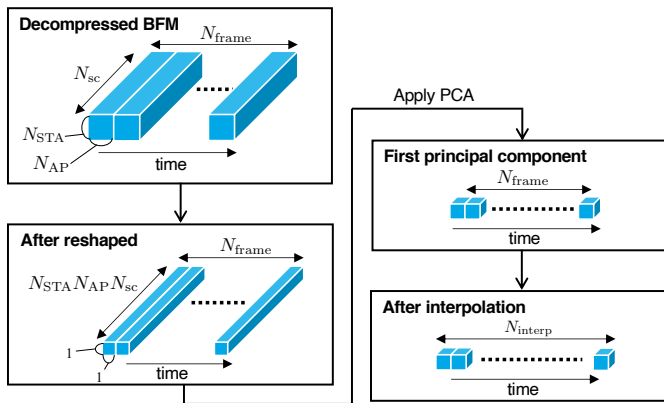


Fig. 2. Data arrangements during the preprocessing. The decompressed BFM data are preprocessed into a one-dimensional vector along time.

Algorithm 1 Respiration detection and estimation

Input: Preprocessed data \mathbf{x}

- 1: Perform DFT on \mathbf{x} , and store the output in \mathbf{y} .
- 2: # Filter by a band-pass filter $L[\cdot]$ in TABLE I
- 3: $\mathbf{y} \leftarrow L[\mathbf{y}]$
- 4: **if** $\max(\mathbf{y})/\text{mean}(\mathbf{y}) < \theta$ **then** # No respiration
- 5: estimation $\leftarrow 0.0$
- 6: **else** # Respiration is detected
- 7: estimation $\leftarrow \text{argmax}(\mathbf{y})$
- 8: **end if**

Output: estimation

to avoid false peak detection, first, we use a band-pass filter to limit the output of the DFT to the frequency range of the human respiration rate. We then calculate the ratio of the peak value to the average value of the DFT output. If the ratio is less than or equal to threshold θ , we estimate it as 0, meaning that there is no respiration or the subject is not breathing. On the other hand, the ratio higher than θ indicates that respiration is detected. During the period the respiration is detected, the respiratory frequency is estimated as the frequency that gives the peak in the DFT signal.

IV. EXPERIMENTAL EVALUATION

In this section, we evaluate the proposed respiratory rate estimation method. First, experimental settings, including parameter and implementation settings, are provided. Second, we show experimental results and some discussions about our preprocessing, DFT output, and estimation. To evaluate the performance of the estimation, we validate the estimation error, which is computed by root mean squared error (RMSE) between the estimation and ground-truth in the time domain.

A. Experimental Setup

We perform our experiments in a room of a concrete building using IEEE 802.11ax WLAN system. The detailed parameter settings of the experiments are listed in TABLE I. The frequency band is 5.2 GHz, and the bandwidth is 80 MHz,

TABLE I
EXPERIMENTAL PARAMETERS

Parameters	Values
Average beamforming feedback interval	0.20 s
Carrier frequency	5.2 GHz
Bandwidth	80 MHz
Number of AP's antennas N_{AP}	4
Number of STA's antennas N_{STA}	4
Number of subcarriers with BFM's N_{sc}	250
Capturing time at each positions and breathing rate	300 s
Time window size	60 s
Interval of linear interpolation	0.1 s
Band-pass filter L range	[10, 50] breaths/minute
Detection threshold θ	5.0

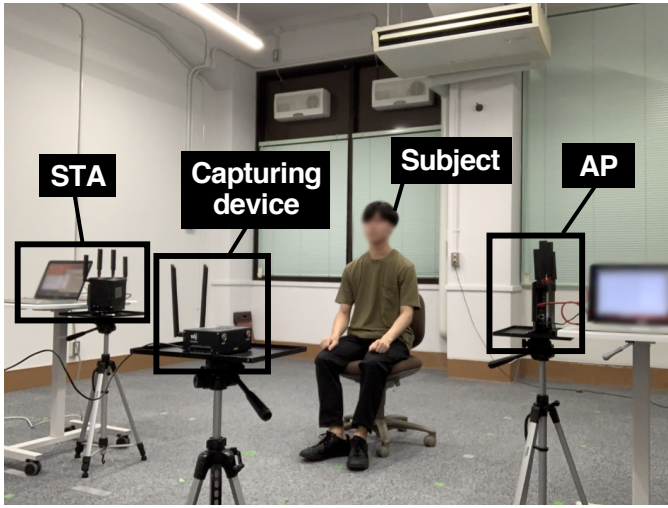
where the subcarrier interval for beamforming feedback in the frequency domain is 312.5 kHz, and $N_{sc} = 250$ BFM's are returned to the AP. Throughout the experiments, we use off-the-shelf WiFi access point WXR-5700AX7S (BUFFALO) as the AP and STA, and Jetson Nano (NVIDIA) with Intel AX200 802.11ax WiFi card as the capturing device. The AP transmits data frames to the STA using the `iperf3` command. The beamforming feedback frames are captured using the capturing device with the `tshark` command, which creates pcap network capture files.

Fig. 3 depicts the experimental setting. The distance between the AP and STA is 2 m, and the subject sits deep on a chair. The room is furnished with desks, chairs, shelves, air conditioners, and ventilation fans. The subject is a 22-year-old-male; he is 1.68 m tall and weighs 56 kg. The height of the chest, the antennas of AP and STA are arranged at the same height.

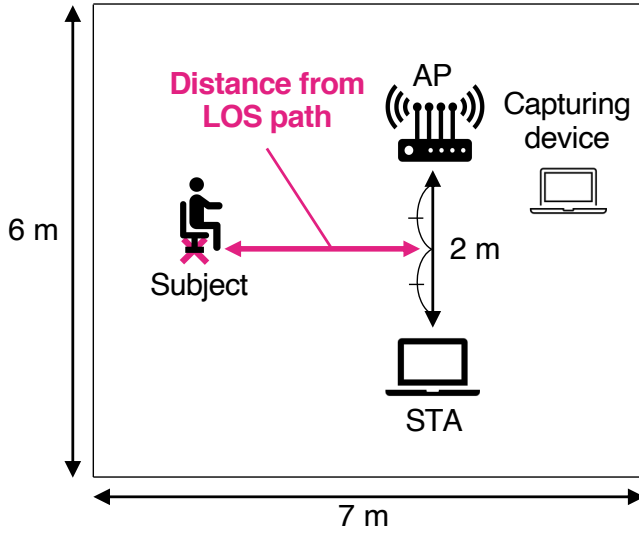
We experimented with the subject at three positions, where the distances from the middle of the line of sight (LOS) path are 1, 2, and 3 m. At each positions, the subject breathes at constant rate of 0, 15, and 20 breaths/minute in sync with a metronome throughout 300 s. The respiratory rate is estimated based on the distance from each position and breathing rate, shifting the time window of 60 s overlapping 1 s with adjacent window. The breathing rate 0 breaths/minute is the state in which the subject is holding breath. As it is impossible for the subject to hold his breath throughout the experiment, we give the subject time to breath in between, which does not significantly affect the respiratory rate estimation because the estimation does not depend on a slight change in the posture of the subject.

B. Results

Preprocessing. Fig. 4 confirms the effectiveness of preprocessing on the decompressed BFM's. Figs. 4(a) and 4(b) show the data after PCA and the contribution rate of each principal component at a distance of 1 m and a breathing rate 15 breaths/minute. Periodic fluctuation has become evident in the first principal component. It has a large contribution rate compared with other principal components. The second and



(a) Photograph of an experiment.



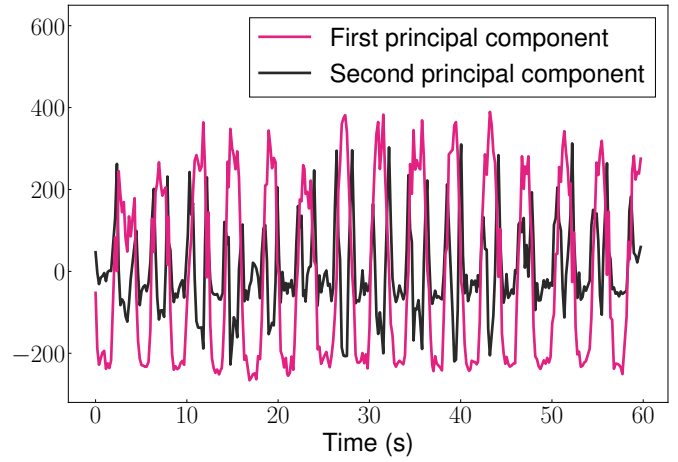
(b) Arrangement of devices.

Fig. 3. Experimental setup. The distance between the AP and STA is 2 m, and one subject is sitting on a chair.

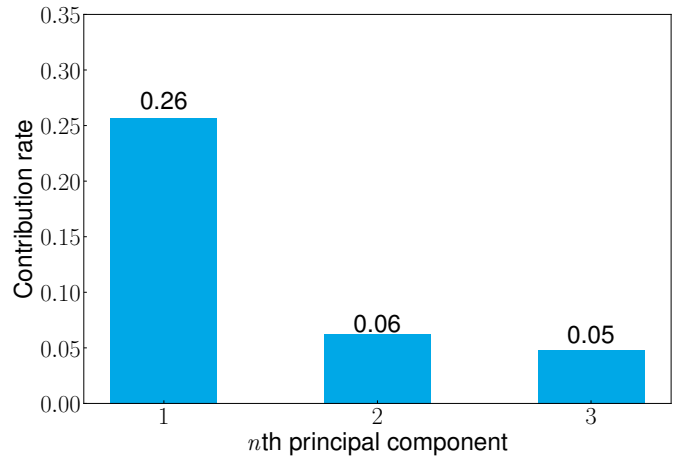
the third principal components possess smaller contribution rate and have been considered to represent the fluctuation of the other channel information, e.g., noises.

DFT Output. Fig. 5 exhibits a clear peak at the frequency of the ground-truth breathing rate of 15 breaths/minute. This figure shows the output of DFT performed on the preprocessed data at 1 m and 15 breaths/minute. By extracting this peak, we can estimate the respiratory rate as discussed below.

Respiratory Rate Estimation. Fig. 6 confirms the feasibility of accurate respiratory rate estimation based on frame capturing. The estimation errors are lower than 3.2 breaths/minute at all the distances from the LOS path. When the subject distance is 1 or 2 m from the LOS path, the estimation error is lower than 0.20 breaths/minute, which would be sufficiently accurate for medical use cases referred



(a) Principal components.



(b) Contribution rate of principal components.

Fig. 4. Effectiveness of preprocessing. Periodic fluctuation owing to respiration becomes evident after PCA, where the first principal component exhibits a large contribution rate compared with other principal components.

in Section I. This result reveals that respiratory rate can be estimated using BFM in the frames captured without firmware modifications nor dedicated WiFi chipsets.

However, the estimation error at a distance of 3 m is higher than those at 1 or 2 m, owing to the signal-to-noise power ratio pertaining to respiratory detection. The received signal power reflected at the subject's chest becomes much weaker than the direct signal along the LOS path. The proposed method may have extracted the fluctuations of channel information in LOS path rather than the effect of breathing motion.

V. CONCLUSION

This paper presented a frame-capture-based respiratory rate estimation method. We proposed an approach using digital signal processing. Specifically, we applied PCA to isolate the effect of chest fluctuation from other channel information, and performed DFT to extract respiratory rate. The experimental results confirmed the feasibility of respiratory rate estimation based on frame capturing, where estimation error is lower

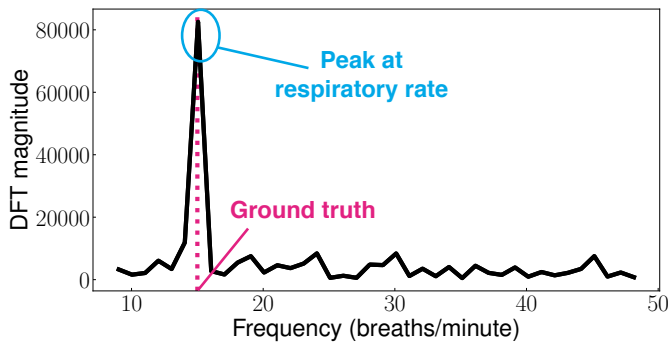


Fig. 5. DFT output. The output exhibits one peak at a frequency corresponding to subject's ground-truth respiratory rate of 15 breaths/minute.

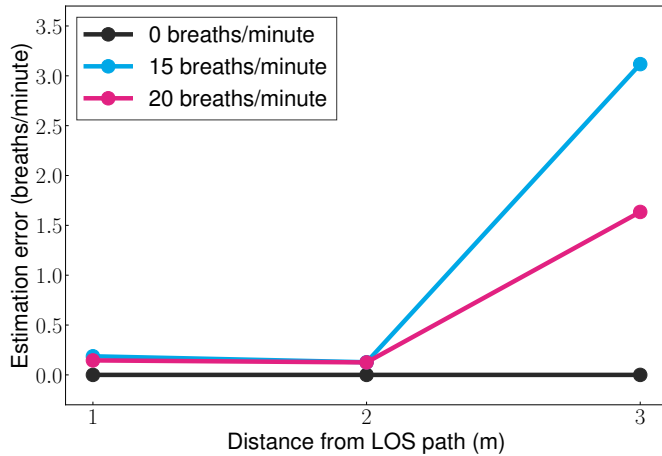


Fig. 6. Estimation error as a function of the distance from the LOS path. The errors are lower than 3.2 breaths/minute at all subject distances. When the distance is smaller than 2 m, the estimation error is lower than 0.20 breaths/minute.

than 3.2 breaths/minute. This implies that the applicability of frame capturing can be extended to various sensing tasks.

ACKNOWLEDGMENT

This work was supported in part by JSPS KAKENHI Grant Number JP18H01442, JP20H04156, and JP20K21793.

REFERENCES

- [1] S. Wan, Y. Xiang, W. Fang, Y. Zheng, B. Li *et al.*, "Clinical features and treatment of COVID-19 patients in northeast Chongqing," *J. Med. Virol.*, vol. 92, no. 7, pp. 797–806, 2020.
- [2] A. D. T. Force, V. Ranieri, G. Rubenfeld, B. Thompson, N. Ferguson *et al.*, "Acute respiratory distress syndrome," *JAMA*, vol. 307, no. 23, pp. 2526–2533, 2012.
- [3] E. Antide, M. Zarudniev, O. Michel, and M. Pelissier, "Comparative study of radar architectures for human vital signs measurement," in *Proc. IEEE Radar Conf. 2020*. IEEE, 2020, pp. 1–6.
- [4] Y. He, Y. Chen, Y. Hu, and B. Zeng, "WiFi vision: Sensing, recognition, and detection with commodity MIMO-OFDM WiFi," *IEEE Internet Things J.*, vol. 7, no. 9, pp. 8296–8317, 2020.
- [5] Y. Ma, G. Zhou, and S. Wang, "WiFi sensing with channel state information: A survey," *ACM Comput. Surv.*, vol. 52, no. 3, pp. 1–36, 2019.
- [6] X. Liu, J. Cao, S. Tang, and J. Wen, "Wi-sleep: Contactless sleep monitoring via WiFi signals," in *Proc. 2014 IEEE Real-Time Syst. Symp.* IEEE, 2014, pp. 346–355.
- [7] X. Liu, J. Cao, S. Tang, J. Wen, and P. Guo, "Contactless respiration monitoring via off-the-shelf WiFi devices," *IEEE Trans. Mobile Comput.*, vol. 15, no. 10, pp. 2466–2479, 2015.
- [8] J. Liu, Y. Wang, Y. Chen, J. Yang, X. Chen, and J. Cheng, "Tracking vital signs during sleep leveraging off-the-shelf WiFi," in *Proc. 16th MobiHoc*, 2015, pp. 267–276.
- [9] "IEEE standard for information technology– telecommunications and information exchange between systems local and metropolitan area networks– specific requirements– part 11: Wireless LAN medium access control (MAC) and physical layer (PHY) specifications– amendment 4: Enhancements for very high throughput for operation in bands below 6 ghz." *IEEE Std 802.11ac-2013 (Amendment to IEEE Std 802.11-2012, as amended by IEEE Std 802.11ae-2012, IEEE Std 802.11aa-2012, and IEEE Std 802.11ad-2012)*, pp. 1–425, 2013.
- [10] "IEEE standard for information technology–telecommunications and information exchange between systems local and metropolitan area networks–specific requirements part 11: Wireless LAN medium access control (MAC) and physical layer (PHY) specifications amendment 1: Enhancements for high-efficiency WLAN," *IEEE Std 802.11ax-2021 (Amendment to IEEE Std 802.11-2020)*, pp. 1–767, 2021.
- [11] T. Fukushima, T. Murakami, H. Abeysekera, S. Saruwatari, and T. Watanabe, "Evaluating indoor localization performance on an IEEE 802.11ac explicit-feedback-based CSI learning system," in *Proc. IEEE VTC2019-Spring*. IEEE, 2019, pp. 1–6.
- [12] M. Miyazaki, S. Ishida, A. Fukuda, T. Murakami, and S. Otsuki, "Initial attempt on outdoor human detection using IEEE 802.11ac WLAN signal," in *Proc. IEEE SAS 2019*. IEEE, 2019, pp. 1–6.
- [13] R. Takahashi, S. Ishida, A. Fukuda, T. Murakami, and S. Otsuki, "DNN-based outdoor NLOS human detection using IEEE 802.11ac WLAN signal," in *Proc. IEEE Sensors 2019*. IEEE, 2019, pp. 1–4.